

Binding induced destruction of an excimer in anthracene-linked benzimidazole diamide: a case toward the selective detection of organic sulfonic acids and metal ions†

Kumares Ghosh,^{*a} Tanushree Sen^a and Amarendra Patra^b

Received (in Gainesville, FL, USA) 24th December 2009, Accepted 17th February 2010

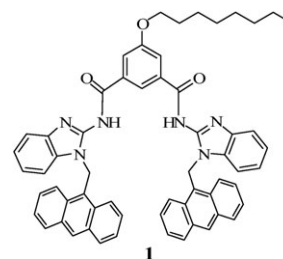
First published as an Advance Article on the web 30th March 2010

DOI: 10.1039/b9nj00789j

A simple anthracene-linked benzimidazole diamide, **1**, has been designed and synthesized. **1** was found to undergo a subtle change in conformation, followed by destruction of the inherently present excimer in the presence of organic sulfonic acids and selective metal ions. Destruction of the excimer did not take place in the presence of carboxylic acids and even stronger trifluoroacetic acid. This finding was taken as a possible tool for distinguishing organic sulfonic acids from carboxylic acids. A similar situation arose in the presence of Cu^{2+} , Co^{2+} and Ni^{2+} , among the other metal ions studied, and the cleft was selective for Cu^{2+} . The binding interaction was followed using ^1H NMR, UV-vis and fluorescence spectroscopic methods.

Introduction

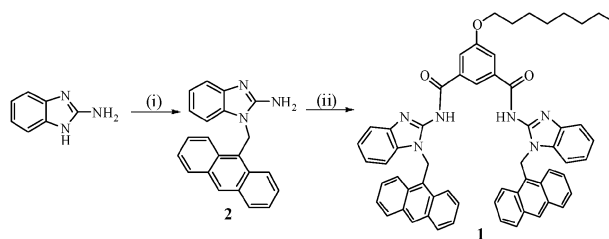
Complexation-induced photophysical changes of molecules have been the prime focus in recent times in the area of supramolecular chemistry. Changes in photophysical behavior of a molecule during complexation may be attributed to the change in various processes, such as electron transfer and excimer/exiplex formation or destruction.¹ Among these, excimer/exiplex formation or destruction is sometimes useful for the identification of different analytes. Such changes occur due to changes in distance between the fluorophores. The coordination of ions, neutral molecules, *etc.* modulates distances by involving a change in conformation. In this respect, protonation-induced changes in conformation of molecules, and hence their supramolecular behavior, is known in the literature.² Molecules of this class provide frameworks within which or between which controlled dynamic structural changes, such as rotations and translations or combinations thereof, can take place.³ Molecular motions can also be triggered by various means (*e.g.* ion binding, electron transfer and light excitation), and can often be reverted by simply removing or reversing the triggering stimulus.³ In order to devise such a system, we report a simple sensory system, **1**, in this paper. Sensor **1** was found to be responsive towards the selective recognition of sulfonic acids over carboxylic acids, and also a few selective metal ions, such as Cu^{2+} , Co^{2+} and Ni^{2+} .



Results and discussion

Benzimidazole-based molecule **1** was synthesized according to Scheme 1. Initially, 2-aminobenzimidazole was reacted with 9-chloromethylantracene in the presence of K_2CO_3 and TBAI catalyst in dry CH_3CN to give amine **2**. A reaction of amine **2** with 5-octyloxyisophthaloyl dichloride in dry THF in the presence of Et_3N at room temperature afforded the desired compound, **1**, in 15% yield. Compound **1** was obtained in low yield due to the poor nucleophilicity of amine **2**. The structure of **1** was established by ^1H NMR, ^{13}C , FTIR and mass analysis.

Compound **1** was designed as a “fluorophore–spacer–receptor–spacer–fluorophore” according to the design principle of a PET (photoinduced electron transfer) system.¹ We performed



Scheme 1 Reagents and conditions: (i) 9-chloromethylantracene, K_2CO_3 , dry CH_3CN ; (ii) 5-octyloxyisophthaloyl dichloride, Et_3N , dry THF.

^a Department of Chemistry, University of Kalyani, Kalyan 741235, India. E-mail: ghosh_k2003@yahoo.co.in; Fax: +91 3325828282; Tel: +91 3325828750

^b Department of Chemistry, University College of Science, 92 A.P.C. Road, Kolkata 700 009, India

† Electronic supplementary information (ESI) available: COSY spectrum (300 MHz) of **1** in CDCl_3 , ROESY spectrum (300 MHz) of **1** in the presence of an equivalent of $\text{CH}_3\text{SO}_3\text{H}$ in CDCl_3 , the effect of the addition of water on the emission spectra of **1** in different solvents, emission spectra of **1** in aq. CH_3CN upon adding 40 equivalents of the acids, absorption spectra of **1** in aq. CH_3CN upon adding 40 equivalents of the acids ($\lambda_{\text{ex}} = 350$ nm) and stoichiometry plots of **1** with metal ions in CH_3CN . See DOI: 10.1039/b9nj00789j

MM2 calculations⁴ on compound **1** to gain an insight into the orientation of the pendant anthracenes. In principle, the anthracenes in **1** may adopt different orientations. The parallel disposition of the anthracenes in the gas phase (Fig. 1a) is energetically less favorable than the other form (Fig. 1b). A study by ¹H NMR of **1** in the absence of acid was performed to understand the conformational behavior of the molecule. A COSY experiment on the molecule indicated correlations of the different protons of **1** (ESI, Fig. S1†). In the absence of strong proton donor acids, the ROESY spectrum of **1** was recorded (Fig. 2). Surprisingly, no cross peaks for the amide protons (H_a) with the isophthaloyl *peri* proton (H_b) and ring proton (H_d) were found. This enabled us to assume that the amides are not perfectly in a plane of the isophthaloyl moiety. However, correlations of isophthaloyl proton H_b with protons H_m and H_c were found (see Fig. 2). This suggests that the anthracenyl motif is close to the diamide core. We also recorded the ROESY spectrum of **1** after adding 2 equivalents of methane sulfonic acid ($\text{CH}_3\text{SO}_3\text{H}$) to a solution in CDCl_3 (ESI, Fig. S2†).

In the presence of $\text{CH}_3\text{SO}_3\text{H}$, the amide protons of **1** moved downfield (Fig. 3; $\Delta\delta = 0.13$ ppm) due to hydrogen bonding interactions of the diamides with the guest acid.

In addition, protonation in presence of $\text{CH}_3\text{SO}_3\text{H}$ is expected to occur on the nitrogen of the benzimidazole ring,⁵ for which a six-membered hydrogen-bonded structure (see Fig. 4) is possible. We were unable to identify this new signal by ¹H NMR, arising due to protonation. Instead, the appearance of a broad peak at 7.98–8.00 ppm was suspected to be due to this consequence (see Fig. 3). Upon protonation, the correlations of the different protons are represented in Fig. 4 (ROESY spectrum; assigned as in ESI, Fig. S2†).

Fluorescence and UV studies

Without having much information from the NMR studies, especially on the conformational behavior of **1**, we performed fluorescence titration experiments. We anticipated that the characteristic emission of the pendant anthracenes, if they remained parallel in **1**, may provide the information by showing a change in intensity or by introducing an excimer at a higher wavelength upon complexation.

For this purpose, the emission of **1** was initially recorded in different solvents. Fig. 5 displays the emission spectra of **1** in

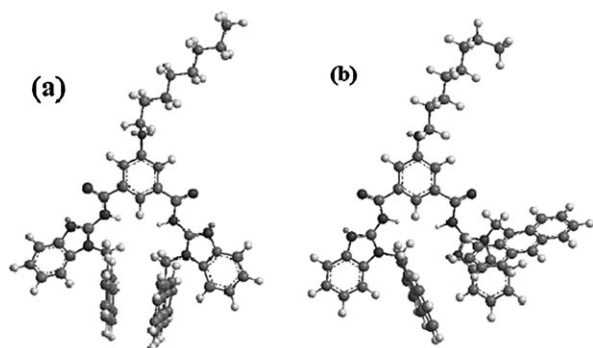


Fig. 1 The MM2 optimized geometries of **1**: (a) $E = 69.96$ kcal mol⁻¹ and (b) $E = 2.52$ kcal mol⁻¹.

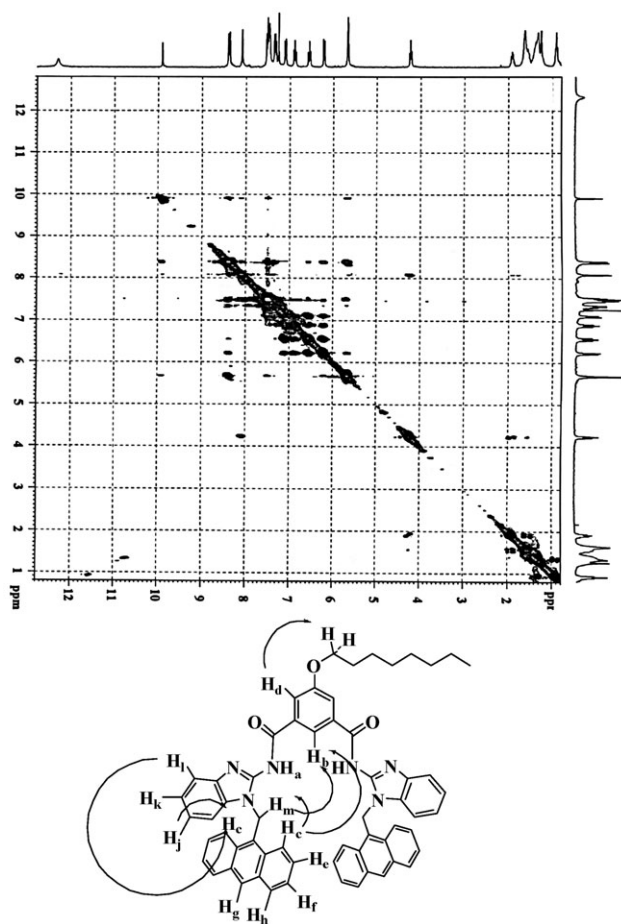


Fig. 2 The ROESY spectrum (300 MHz) of **1** in CDCl_3 .

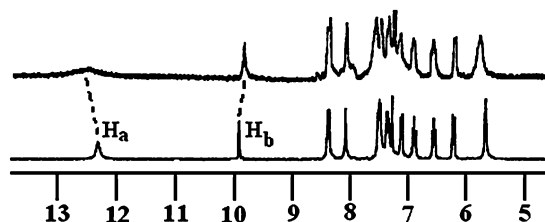


Fig. 3 Partial ¹H NMR spectra (300 MHz) of (a) **1** ($c = 1.03 \times 10^{-2}$ M) and (b) its 1:2 (host:guest) complex with $\text{CH}_3\text{SO}_3\text{H}$.

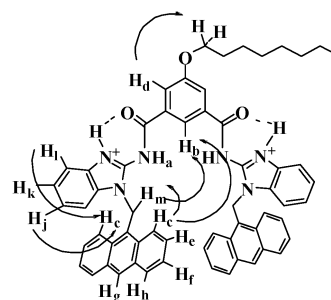


Fig. 4 Correlations of the different protons in **1** after protonation.

CHCl_3 , CH_3CN , THF and MeOH solvents when excited at 350 nm. In all cases, an emission at a higher wavelength (520 nm) was observed, along with a structured emission centered at 420 nm.

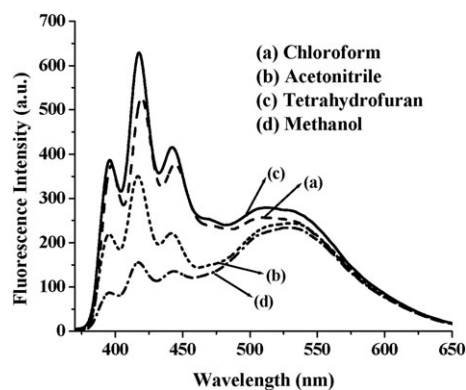


Fig. 5 Emission spectra of **1** ($c = 8.87 \times 10^{-5}$ M) in different solvents.

It is evident from Fig. 5 that the intensity of the emission at 520 nm, attributed to the intramolecular excimer between the pendant anthracenes, is merely affected by the changing polarity of the solvent. However, the monomer emission of **1**, centered at 420 nm, suffers a drastic change in intensity with solvent polarity. This is assumed to be due to the role of the solvents, which solvate the diamide core to different extents. Therefore, it is quite reasonable that if any analyte that has the tendency to interact *via* non-covalent forces is present in the organic solvent, it will certainly cause a change in intensity of the emissions at 420 and 520 nm. With this in mind, we first studied the influence of the small molecule water⁶ on the emission spectrum of **1**. ESI, Fig. S3† highlights the change in emission of **1** when water is added in different proportions to solutions of **1** in CH_3CN , CHCl_3 , CH_3OH and THF.

It is of worth noting that the change in excimer emission is significant in aq. CH_3OH (Fig. 6). Such a significant change in emission of the peak at 520 nm is due to hydrogen bonding interactions of water at the diamide core of **1**, for which the pendant anthracenes are pulled closer. Due to the immiscibility of water in CHCl_3 , this change was minor in this solvent. In THF, it was also found to be less because of its competitive role in the formation of hydrogen bonds with the amides. This notable observation is thus interesting in the realm of detecting the presence of water in organic solvents, particularly in CH_3OH and CH_3CN . After observing the effect of water on the emission of **1**, we thoroughly investigated the emission properties of **1** in CHCl_3 upon gradually adding solutions of different acids, such as organic sulfonic acids, carboxylic acids, *etc.*

A chloroform solution of **1** was excited at 350 nm, and the emission was monitored at 419 nm upon adding different acids, such as acetic acid, (*S*)-mandelic acid, trifluoroacetic acid, methanesulfonic acid, *p*-toluenesulfonic acid, *etc.* Fig. 7, for example, represents the fluorescence titration spectra of **1** in the presence of *p*-toluenesulfonic acid.

Importantly, the change in emission was considerable in the presence of methanesulfonic acid and *p*-toluenesulfonic acid. For carboxylic acids, such as acetic acid or (*S*)-mandelic acid, the change in emission of the excimer was comparatively less compared to the case of the sulfonic acids. The emission was less perturbed even upon adding trifluoroacetic acid (TFA). Fig. 8, in this regard, provides a comparison of the emission

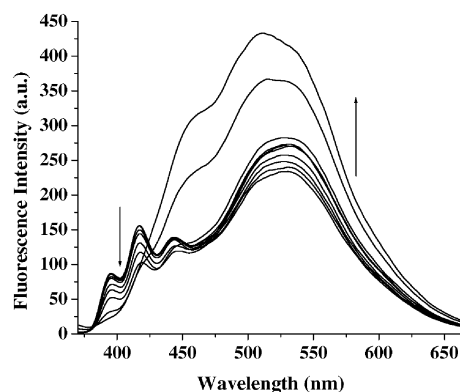


Fig. 6 The effect of adding of water on the emission spectra of **1** in CH_3OH .

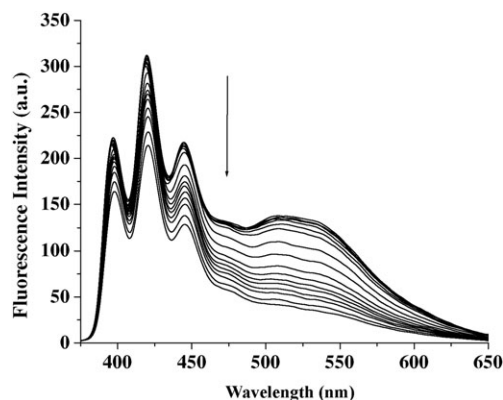


Fig. 7 Fluorescence titration spectra of **1** ($c = 9.95 \times 10^{-6}$ M) in CHCl_3 upon adding *p*-toluene sulfonic acid ($\lambda_{\text{ex}} = 350$ nm).

spectra of **1** in the presence of 40 equivalents of each particular acid.

Therefore, this observation is useful for distinguishing sulfonic acids from carboxylic acids in the less polar solvent CHCl_3 . We believe that methane sulfonic acid and *p*-toluene sulfonic acid, being stronger acids, will induce protonation on the benzimidazole moieties and form ion pairs according to Fig. 9. Such ion pair formation is also equally probable with trifluoroacetic acid (Fig. 9). Weaker acids, such as acetic acid

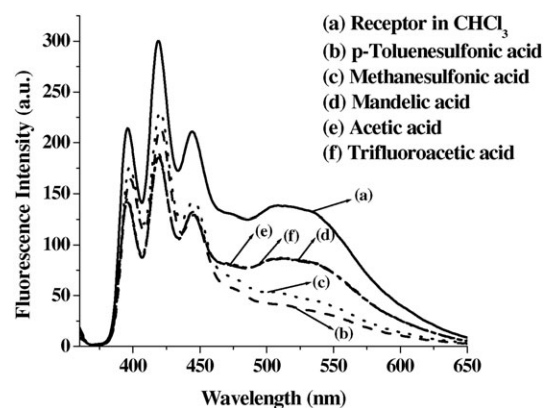


Fig. 8 Emission spectra of **1** ($c = 9.95 \times 10^{-6}$ M) in CHCl_3 upon adding 40 equivalents of each acid ($\lambda_{\text{ex}} = 350$ nm).

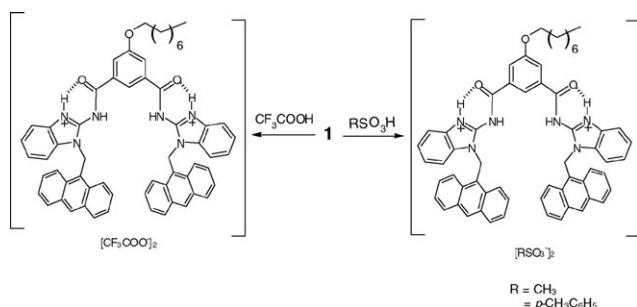


Fig. 9 Suggested structures of ion pairs of **1** in the presence of sulfonic acids and TFA.

and (*S*)-mandelic acid, are unable to cause such facile protonation in the less polar solvent CHCl_3 and thus exhibit a small perturbation in the emission *via* hydrogen-bonding interactions. We consider that the differential change in emission of excimer in **1** is due to the formation of different ion pairs in solution. In the case of methane sulfonic acid and *p*-toluene sulfonic acid, the sulfonate anions play a key role in quenching the emission, either by hydrogen-bonding or by a bimolecular collision effect that destroys the excimer completely. This is less in magnitude in case of the trifluoroacetate anion. We further believe that the sulfonate ion, being tetrahedral in shape, demands more space than the planar carboxylate ion for its hydrogen bonding interaction into the diamide core of **1**, and accordingly induces a change in the distance between the anthracenes, for which parallel stacking of the two anthracene units is no longer possible.

A concurrent change in the absorption of **1** was also recorded in the presence of the same acids in CHCl_3 (Fig. 10). During titration with a particular acid, the absorbance at 323 nm decreased steadily. The peak at 323 nm, assigned to the benzimidazole motif, partially buried the absorption peak of the anthracene at around 370 nm. A close inspection of the spectral change indicates that the change in absorbance for anthracene was minor during the titrations, and thus compound **1** fulfilled the criteria of a PET system.

Only the benzimidazole motif suffered a greater change in absorbance, and thus confirmed its participation in interactions in the ground state. For example, Fig. 11 represents the change in the UV spectrum of **1** upon titration with methane sulfonic

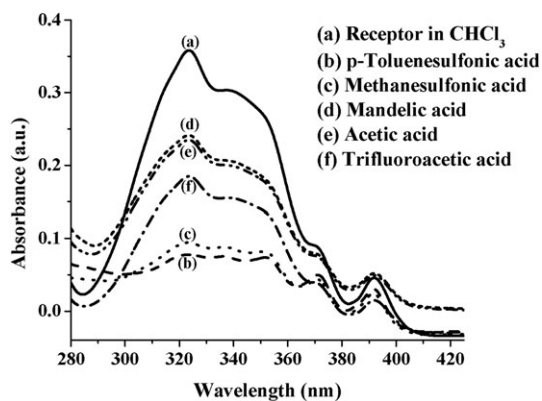


Fig. 10 Absorption spectra of **1** ($c = 9.95 \times 10^{-6}$ M) in CHCl_3 upon adding 40 equivalents of each acid.

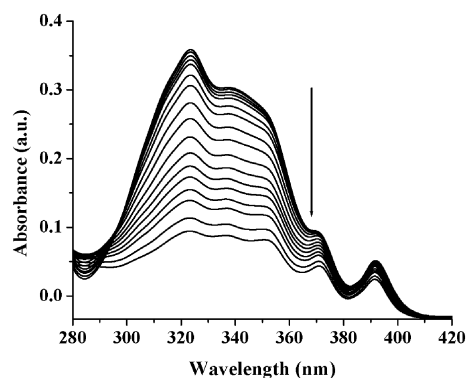


Fig. 11 UV titration spectra of **1** ($c = 9.95 \times 10^{-6}$ M) in CHCl_3 upon adding methane sulfonic acid.

acid. To realize the interaction stabilities of **1** with the acids, we tried to determine the binding constant values in CHCl_3 using both fluorescence and UV-vis titration results. However, no satisfactory values were obtained to report.

We also carried out the similar experiments (fluorescence and UV) with **1** using the same guests in aq. CH_3CN ($\text{CH}_3\text{CN}:\text{H}_2\text{O} = 4:1$ v/v). Importantly, in each case, the degree of change in emission of the excimer in **1** was almost the same magnitude; this was even true in the ground state. ESI, Figs. S4 and S5† represent the emission and absorption spectra of **1** in the presence of 40 equivalents of the acids previously mentioned in this study. The similar effect of all the acids on the emission/absorption spectrum of **1**, we propose, is due to the effect of water, which blocks the diamide core *via* hydrogen-bonding interactions and nullifies the hydrogen-bonding effect of anions, such as sulfonates and carboxylates.

However, the above thorough study reveals that the excimer of **1** can be destroyed successfully by adding a stronger acid, and in the present case, organic sulfonic acids are able to do this. In comparison, carboxylic acids are unable to induce the conformational change so effectively. Thus, this observation led us to discriminate sulfonic acids from carboxylic acids. Sulfonic acids are typically much stronger acids than their carboxylic acid equivalents, and have the unique tendency to bind to proteins and carbohydrates tightly; most “washable” dyes are sulfonic acids (or have the functional sulfonyl group in them) for this reason. They are also used as catalysts and intermediates for a number of different products.^{7a} Sulfonic acids and their salts (sulfonates) are used extensively in a diverse range of products, such as detergents, antibacterial drugs, sulfa drugs, anion exchange resins (water purification) and dyes. Methane sulfonic and *p*-toluene sulfonic acids are also reagents that are regularly used in organic chemistry.^{7b,c,d} Therefore, the selective sensing of organic sulfonic acids in organic solvents is an important aspect in analytical chemistry, and the present report is undoubtedly useful in this respect. In order to explore the possibility of using this simple sensory system (**1**), we further investigated its metal interaction properties by monitoring the intensity of the excimer.

A similar situation, *i.e.* the destruction of the excimer of **1**, occurred when different metal ions were added to a solution of **1**. The nitrogen centers present in the cleft of **1** are prone to coordinating metal ions as possible donors. The coordination

of metal ions in the cleft will thus, in principle, destroy the facial organization of the anthracene and bring substantial photophysical changes that lead to the destruction of the inherently-present excimer. With this in mind, we additionally carried out spectroscopic studies of **1** with several metal ions of biological significance.

Complexation of metal ions

The metal ion complexation of **1** was studied in CH₃CN. Compound **1** ($c = 3.3 \times 10^{-6}$ M) in CH₃CN showed a monomeric emission centered at 414 nm when excited at 350 nm, accompanied by a broad intense band at 520 nm due to intramolecular excimer. Upon adding increasing amounts of metal ions to solutions of **1**, the emissions for both the monomer and excimer decreased progressively. The initial addition of metal ions to solutions of **1** caused substantial changes in emission; excess additions little altered the emission.

Interestingly, the monomer emission for the anthracene moiety significantly decreased in the presence of a large excess of some of the metal ions, leading to the complete destruction of the excimer at 520 nm. Such a trend was observed in the case of Cu²⁺, Co²⁺ and Ni²⁺ ions during complexation in CH₃CN (Fig. 12). Fig. 13, for example, shows the change in the emission spectrum of **1** in the presence of 6 equivalents of Cu²⁺. During the interaction, the quenching of the emission is mentionable, and in this regard the paramagnetic effect of the Cu²⁺ cannot be excluded.⁸

However, from Fig. 12, it is clear that the excimer emission intensity is greatly changed by the presence of Cu²⁺, Co²⁺ and Ni²⁺ ions, in comparison to the rest of the metal ions, namely Mn²⁺, Zn²⁺, Cd²⁺, Ag⁺ and Pb²⁺. These findings are diagnostic for the detection of Cu²⁺, Co²⁺ and Ni²⁺ metal ions from the others present in the study. We believe that this high affinity of **1** for Cu²⁺, Co²⁺ and Ni²⁺ is attributed to the comfortable mode of binding of the metal ions at the diamide core, satisfying the possible coordination number with geometrical complementarity.

Stern–Volmer plots, associated with the quenching of the emission, induced by coordination of metal ions, are displayed in Fig. 14. From the plots, it is clear that the cleft of **1** has a greater selectivity for Cu²⁺ ions. In this respect, it is known that among the various transition metal ions, copper ions

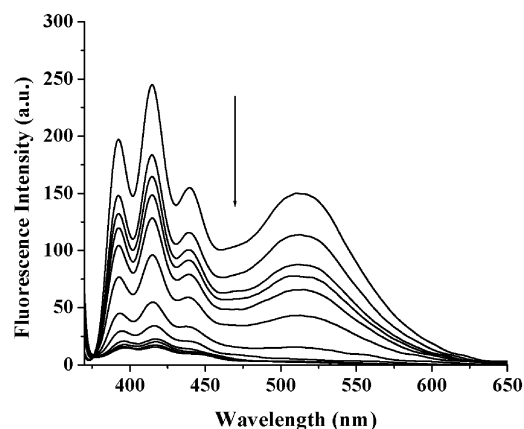


Fig. 13 The emission spectrum of **1** ($c = 3.3 \times 10^{-6}$ M) in CH₃CN upon adding 6 equivalents of Cu²⁺ ions ($\lambda_{\text{ex}} = 350$ nm).

draw significant attention due to their crucial role in biological systems. This metal ion causes significant environmental pollution and also serves as a catalytic cofactor for a variety of metalloenzymes.⁹ However, exposure to a high level of copper, even for a short period of time, can cause gastrointestinal disturbance, while long-term exposure can cause liver or kidney damage.¹⁰ For these reasons, the past few years have witnessed a number of reports on the design and synthesis of fluorescent sensors for the detection of Cu²⁺ ions.^{10a,c11} In this report, receptor **1** is an example for the selective detection of Cu²⁺ ions.

The ground state interaction properties of **1** towards these same metal ions were also investigated in CH₃CN. Upon the successive addition of these metal ions to solutions of **1**, the absorption intensity due to the anthracene motif at 370 and 390 nm gradually increased, whereas the absorption peak at 320 nm for the benzimidazole moiety decreased, giving rise to an isosbestic point at 356 nm. The generation of an isosbestic point during the titration indicates the formation of a new species in solution. This type of interesting behavior for **1** was observed for Cu²⁺, Co²⁺ and Ni²⁺. In this context, Fig. 15 represents the change in absorption of **1** upon titration with Cu²⁺ and Co²⁺ ions in CH₃CN.

In order to gain an insight into the binding efficiency of the cleft of **1** with the metal ions, we determined binding constant

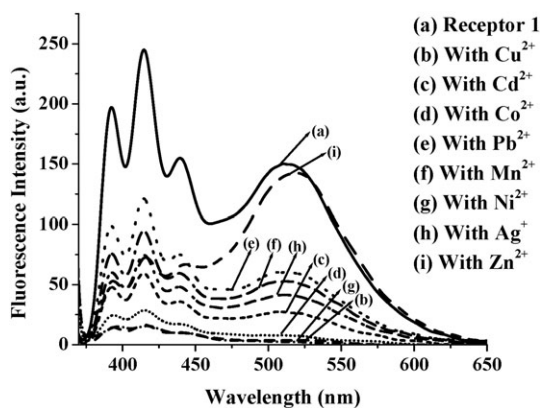


Fig. 12 The emission spectrum of **1** ($c = 3.3 \times 10^{-6}$ M) in CH₃CN upon adding 6 equivalents of various metal ions $\lambda_{\text{ex}} = 350$ nm).

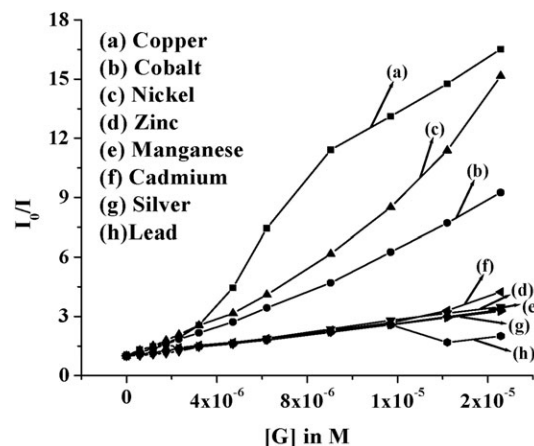


Fig. 14 Stern–Volmer plots of **1** with different metal ions in CH₃CN.

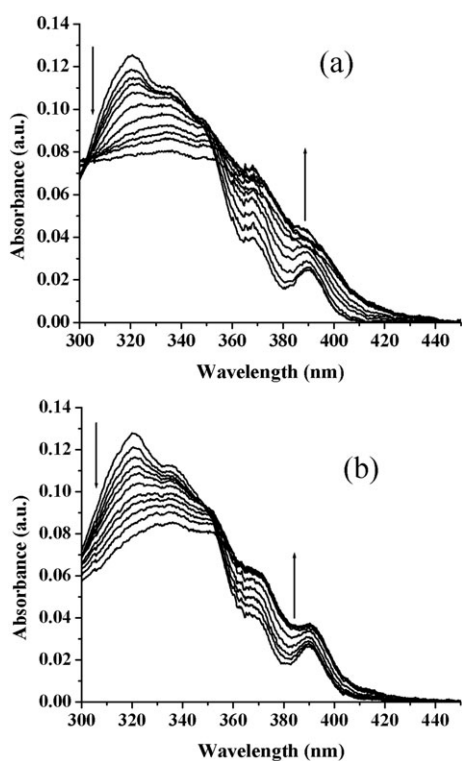


Fig. 15 UV titration spectra of **1** ($c = 3.3 \times 10^{-6}$ M) in CH_3CN upon adding (a) Cu^{2+} and (b) Co^{2+} ions.

values using the emission data (Table 1).¹² Among all the metal ions in Table 1, Cu^{2+} showed the highest affinity for **1**. The binding stoichiometry of the complexes was 1 : 1, as confirmed from the break of the titration curves (ESI, Fig. S6†). To examine the reversibility of the binding of **1** to these metal ions, aqueous solutions of EDTA disodium were added to solutions of **1** and complexed metal ions in CH_3CN . As expected, the fluorescence signal for the excimer was partially revived in the case of **1** with Cu^{2+} , as shown in Fig. 16, demonstrating that the binding is chemically reversible and the equilibrium favourably lies to the left ($\text{1} \cdot \text{Cu}^{2+}$).

Conclusion

In conclusion, we have developed a new fluorescent sensor for the selective detection of organic sulfonic acids, and also Cu^{2+} ions, on the basis of the binding-induced destruction of an excimer between two closely spaced anthracenes. Such a signal transduction mode in **1** might be useful for the design of new fluorophore-based sensory systems. Further progress in this respect is under way in our laboratory.

Experimental

Syntheses

1-(Anthracen-9-ylmethyl)-1H-benzodimidazol-2-amine (2). 2-Aminobenzimidazole (0.2 g, 0.001 mol) was stirred with K_2CO_3 (0.1 g) in dry CH_3CN (15 mL) for 15 min at rt. To the suspension was added 9-chloromethylantracene (0.34 g, 0.001 mol) and a catalytic amount of TBAI. The reaction

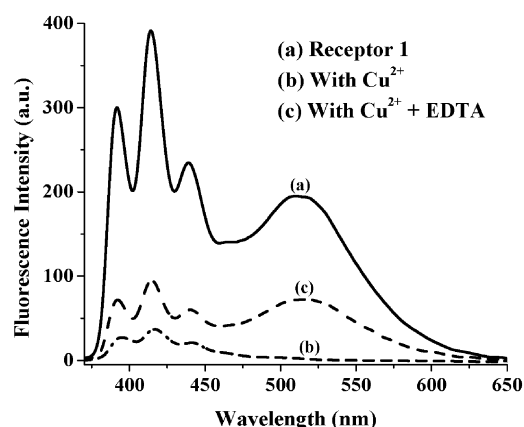


Fig. 16 The influence of adding an EDTA disodium solution to a solution of **1** with complexed Cu^{2+} ions in CH_3CN .

Table 1 Binding constant values for **1** with different metal ions, obtained by fluorescence methods

Guests ^a	Log K_a ^b
Cu^{2+}	6.05
Co^{2+}	5.47
Ni^{2+}	5.65
Cd^{2+}	5.30
Mn^{2+}	5.15
Zn^{2+}	5.12
Pb^{2+}	5.2
Ag^+	5.19

^a Perchlorate salts were taken. ^b Errors were $\leq 10\%$.

mixture was stirred for 8 h. The solvent was removed under reduced pressure and the residue dissolved in CHCl_3 containing 2% CH_3OH (30 mL). The organic layer was washed with water (2×15 mL), left over anhydrous Na_2SO_4 for 10 min and concentrated under vacuum. The crude mass was purified by column chromatography using 40% ethyl acetate in petroleum ether (60–80 °C) as the eluent. Amine **2** was isolated as a yellow solid (0.22 g, 46% yield). Mp. 190 °C.

¹H NMR (400 MHz, CDCl_3) δ 8.54 (s, 1H), 8.22 (d, 2H, $J = 8.4$ Hz), 8.04 (d, 2H, $J = 7.9$ Hz), 7.51–7.45 (m, 4H), 7.34 (d, 1H, $J = 7.8$ Hz), 7.06 (t, 1H, $J = 7.4$ Hz), 6.98–6.90 (m, 2H), 6.05 (s, 2H), 4.56 (br s, amine $-\text{NH}-$, 2H). FTIR: ν/cm^{-1} (in KBr) 3354, 2921, 2851, 1612, 1571, 1467, 1234.

N^1, N^3 -Bis(1-(anthracen-9-ylmethyl)-1H-benzodimidazol-2-yl)-5-(octyloxy)isophthalamide (1). To a stirred solution of 5-octyloxyisophthaloyl dichloride (0.27 g, 0.001 mol) in dry THF (10 mL) was added dropwise with constant stirring a solution of amine **2** (0.66 g, 0.002 mol) along with Et_3N (0.3 mL, 0.002 mol) in dry THF (15 mL). The reaction mixture was stirred overnight at rt. The solvent was evaporated under reduced pressure, washed with 20% NaHCO_3 solution and extracted with CHCl_3 (3×20 mL). The organic layer was washed with water (20 mL), dried over anhydrous Na_2SO_4 and concentrated. The residue was collected and purified by column chromatography using 3% CH_3OH in CHCl_3 as the eluent. Receptor **1** was obtained as a light pink solid (0.3 g, 15% yield). Mp. 168–172 °C.

^1H NMR (400 MHz, CDCl_3) δ 12.28 (s, amide NH, 2H), 9.89 (s, 1H), 8.38 (d, 4H, $J = 8.9$ Hz), 8.07 (s, 2H), 7.52–7.45 (m, 10H), 7.32 (t, 4H, $J = 7.4$ Hz), 7.09 (d, 2H, $J = 7.8$ Hz), 6.88 (t, 2H, $J = 7.7$ Hz), 6.55 (t, 2H, $J = 7.8$ Hz), 6.21 (d, 2H, $J = 8.2$ Hz), 5.66 (s, 4H), 4.23 (t, 2H, $J = 6.5$ Hz), 1.93–1.88 (m, 2H), 1.39–1.24 (m, 10H), 0.91 (t, 3H, $J = 6.8$ Hz). ^{13}C (125 MHz, CDCl_3) δ 176.3, 159.6, 153.4, 139.5, 130.5, 130.3, 129.6, 129.5, 128.6, 128.2, 126.6, 124.8, 124.4, 124.3, 123.7, 122.7, 122.5, 117.9, 111.0, 110.7, 68.6, 38.8, 31.9, 29.43, 29.37, 29.31, 26.1, 22.7, 14.1. FTIR (ν/cm^{-1} , KBr): 3275, 2927, 2854, 1625, 1562, 1478, 1362, 1338, 1286. Mass (ESI): 904.8 $[\text{M} + \text{H}]^+$, 926.9 $[\text{M} + \text{Na}]^+$.

Acknowledgements

We thank DST, Government of India for providing facilities in the department under the DST FIST program. T. S. thanks CSIR, Government of India for a fellowship.

References

- 1 A. P. de Silva, H. Q. N. Gunaratne, T. Gunnlaugsson, A. J. M. Huxley, C. P. McCoy, J. T. Rademacher and T. E. Rice, *Chem. Rev.*, 1997, **97**, 1515.
- 2 (a) P. S. Corbin and S. C. Zimmermann, *J. Am. Chem. Soc.*, 2000, **122**, 3779; (b) M. Barboiu and J.-M. Lehn, *Proc. Natl. Acad. Sci. U. S. A.*, 2002, **99**, 5201.
- 3 (a) For reviews, see: Special issue on Molecular Mechanics, ed. J. F. Stoddart, *Acc. Chem. Res.*, 2001, **34**, pp. 409; (b) V. Balzani, F. Credi, M. Raymo and J. F. Stoddart, *Angew. Chem.*, 2000, **112**, 3484; V. Balzani, F. Credi, M. Raymo and J. F. Stoddart, *Angew. Chem., Int. Ed.*, 2000, **39**, 3348.
- 4 Energy optimization was performed using CS Chem 3D, version 7.0.
- 5 C. J. Matthews, V. Broughton, G. Bernardinelli, X. Melich, G. Brand, A. C. Willis and A. F. Williams, *New J. Chem.*, 2003, **27**, 354.
- 6 A. J. Wilson, J. Hong, S. Fletcher and A. D. Hamilton, *Org. Biomol. Chem.*, 2007, **5**, 276.
- 7 (a) T. Yamamoto, *Chem. Lett.*, 2003, **32**, 334; (b) C. Long, Q.-X. Zhang, A.-M. Li and J.-L. Chen, *Chin. J. Polym. Sci.*, 2004, **22**, 535 and references cited therein; (c) J. A. Titus, R. Haugland, S. O. Sharrow and D. M. Segal, *J. Immunol. Methods*, 1982, **50**, 193; (d) C. Lefevre, H. C. Kang, R. P. Haugland, N. Malekzadeh, S. Arttamangkul and R. P. Haugland, *Bioconjugate Chem.*, 1996, **7**, 482.
- 8 S. Kaur and S. Kumar, *Tetrahedron Lett.*, 2004, **45**, 5081.
- 9 (a) G. Multhaup, A. Schlicksupp, L. Hess, D. Beher, T. Ruppert, C. L. Masters and K. Beyreuther, *Science*, 1996, **271**, 1406; (b) R. A. Løvstad, *BioMetals*, 2004, **17**, 111; (c) D. G. Barceloux and D. Barceloux, *Clin. Toxicol.*, 1999, **37**, 217; (d) B. Sarkar, in *Metal Ions in Biological Systems*, ed. H. Siegel and A. Siegel, Marcel Dekker, New York, 1981, vol. 12, pp. 233; (e) E. L. Que, D. W. Domaille and C. J. Chang, *Chem. Rev.*, 2008, **108**, 1517.
- 10 (a) H. S. Jung, M. Park, D. Y. Han, E. Kim, C. Lee, S. Ham and J. S. Kim, *Org. Lett.*, 2009, **11**, 3378; (b) B. Nisar Ahamed, I. Ravikumar and P. Ghosh, *New J. Chem.*, 2009, **33**, 1825; (c) Y. Zheng, K. M. Gattas-Asfura, V. Konka and R. M. Leblanc, *Chem. Commun.*, 2002, 2350; (d) H. J. Kim, J. Hong, A. Hong, S. Ham, J. H. Lee and J. S. Kim, *Org. Lett.*, 2008, **10**, 1963; (e) H. S. Jung, P. S. Kwon, J. W. Lee, J. L. Kim, C. S. Hong, J. W. Kim, S. Yan, J. Y. Lee, J. H. Lee, T. Joo and J. S. Kim, *J. Am. Chem. Soc.*, 2009, **131**, 2008; (f) Y.-Q. Weng, F. Yue, Y.-R. Zhong and B.-H. Ye, *Inorg. Chem.*, 2007, **46**, 7749; (g) R. Martínez, F. Zapata, A. Caballero, A. Espinosa, A. Tarraga and P. Molina, *Org. Lett.*, 2006, **8**, 3235.
- 11 (a) Y. Xiang, A. Tong, P. Jin and Y. Ju, *Org. Lett.*, 2006, **8**, 2863; (b) S. H. Kim, J. S. Kim, S. M. Park and S.-K. Chang, *Org. Lett.*, 2006, **8**, 371; (c) X. Qi, E. J. Jun, L. Xu, S.-J. Kim, J. S. J. Hong, Y. J. Yoon and J. Yoon, *J. Org. Chem.*, 2006, **71**, 2881.
- 12 P. T. Chou, G. R. Wu, C. Y. Wei, C. C. Cheng, C. P. Chang and F. T. Hung, *J. Phys. Chem. B*, 2000, **104**, 7818.